AIAA-2002-0194
Phase-Resolved Chemiluminescence of an Acoustically Forced Jet Flame at Frequencies < 60 Hz

W. Pun, A. Ratner, and F.E.C. Culick
California Institute of Technology
Pasadena, CA

40th AIAA Aerospace Sciences Meeting & Exhibit

14-17 January 2002 / Reno, NV

PHASE-RESOLVED CHEMILUMINESCENCE OF AN ACOUSTICALLY FORCED JET FLAME AT FREQUENCIES <60 HZ

Winston Pun*, Albert Ratner†, and F. E. C. Culick‡
Mechanical Engineering and Jet Propulsion
California Institute of Technology
Pasadena, CA 91125
Tel: (626) 395-4783

Abstract –The California Institute of Technology's Combustion Acoustics Facility is used to measure the response of a partially premixed jet flame to acoustic forcing at frequencies ranging from 22 Hz to 55 Hz. The facility generates bulk acoustic modes that simulate unstable combustor conditions. This same facility and burner has been previously used to measure the phase-resolved response of the OH PLIF field. In this experiment, phase-resolved chemiluminescence measurements are recorded and analyzed. Flame base oscillations are quantified and compared for two different burner configurations. The chemiluminescence also shows that frequencies that exhibit stronger acoustic coupling to the flame tend to have decreased luminosity in the flame stabilization zone, while frequencies with weaker coupling tend to produce greater luminosity at the base of the flame.

INTRODUCTION

In combustion experiments, a now common method of determining the reaction zone is to image the light emitted in the combustion zone (McManus et al., 1995). Of particular importance are C_2, CH, and OH radicals, since they are produced as intermediaries of the combustion process. Hurle et al. (1968) established the linearity between the radiation emitted and the volumetric heat release. Numerous studies involving naturally occurring combustion instabilities have taken place using this relationship (Samiengo et al., 1993; Shih et al., 1996; Broda et al., 1998). Flame radiation measurements by Chen et al. (1993) utilized a system that could inject acoustic waves at various frequencies, but achieved poor spatial resolution through a masked photomultiplier tube.

The measurements taken by Sterling (1987) also used a masked PMT to obtain spatial resolution, and were subsequently improved upon by Zsak (1993) and Kendrick (1995), with the introduction of the Hycam (high-speed film camera) providing two-dimensional spatial resolution. In this work, advances in imaging technology are utilized to further simplify measurements by employing a digital high-speed video camera. This provides temporally and spatially resolved measurements of the flame chemiluminescence in cases where the flame is subjected to a forced acoustic field.

EXPERIMENT APPARATUS AND CONFIGURATION

The configuration of the acoustic test chamber is shown in Figure 1. The acoustic driving system appears in the upper portion of the chamber, and is mounted above the acoustic cavity on the outer quartz tube. The driving portion is made of a large tubular stainless steel section in the shape of a cross, approximately 12 inches in diameter, which extends the overall length of the acoustic chamber an additional 24 inches. The exhaust section is open to the atmosphere, providing an acoustically open exit condition. A pair of acoustic drivers are sealed to a pair of air jet film cooling rings (to prevent failure of the drivers), which are in turn sealed to opposite sides of the steel structure. The acoustic drivers are 12 inch subwoofers (Cerwin-Vega model Vega 124), with a sensitivity of 1 W @ 1 m of 94 dB, and a continuous power handling capacity of 400 W. A 1000 W power amplifier (Mackie M1400i) and a function generator (Wavetek 171) provide the power and signal to the acoustic drivers. Significant power is required to provide reasonable amplitude

* Postdoctoral Scholar, Mechanical Engineering
† Postdoctoral Scholar, Graduate Aeronautical Laboratories
‡ Richard L. and Dorothy M. Hayman Professor of Mechanical Engineering and Professor of Jet Propulsion.

This work was sponsored partly by the California Institute of Technology; partly by a grant under the Defense University Research Instrumentation Program, provided by the Air Force Office of Scientific Research; partly by the Department of Energy, AGTSR Program; and partly by ENEL.

pressure oscillations. The amplitude of the fundamental driving mode is actively controlled by custom-designed electronics, which measure the pressure in the acoustic chamber at the burner with a pressure transducer (PCB 106B50), and appropriately scale the power output of the amplifier driving the speakers. The signal from the transducer is notch-filtered to ensure the intended driving mode is correctly amplified or attenuated.

The acoustic cavity consists of an aluminum ring, closed at the bottom end. It has two sets of inlet louvers cut on opposing sides to allow air to flow into the tube, while providing an acoustically closed end condition. A large diameter-matched quartz tube rests in a thin register on the aluminum ring, and extends for an additional 42 inches. This design allows for a variety of different flameholder configurations to be easily tested. Two burner designs are tested in this apparatus, an aerodynamically stabilized and bluff-body stabilized flame (Pun et al, 2000).

For aerodynamic stabilization, the flame is stabilized above the recirculation zone created as the flow exits the eductor, and expands into the 4.5 inch tall burner tube. In the bluff-body stabilized burner, two additional tabs (constructed of machinable ceramic) are provided in the stabilization zone, which can provide a stronger recirculation zone for the flame to attach itself. The overall height of the burner is matched to the aerodynamically stabilized configuration.

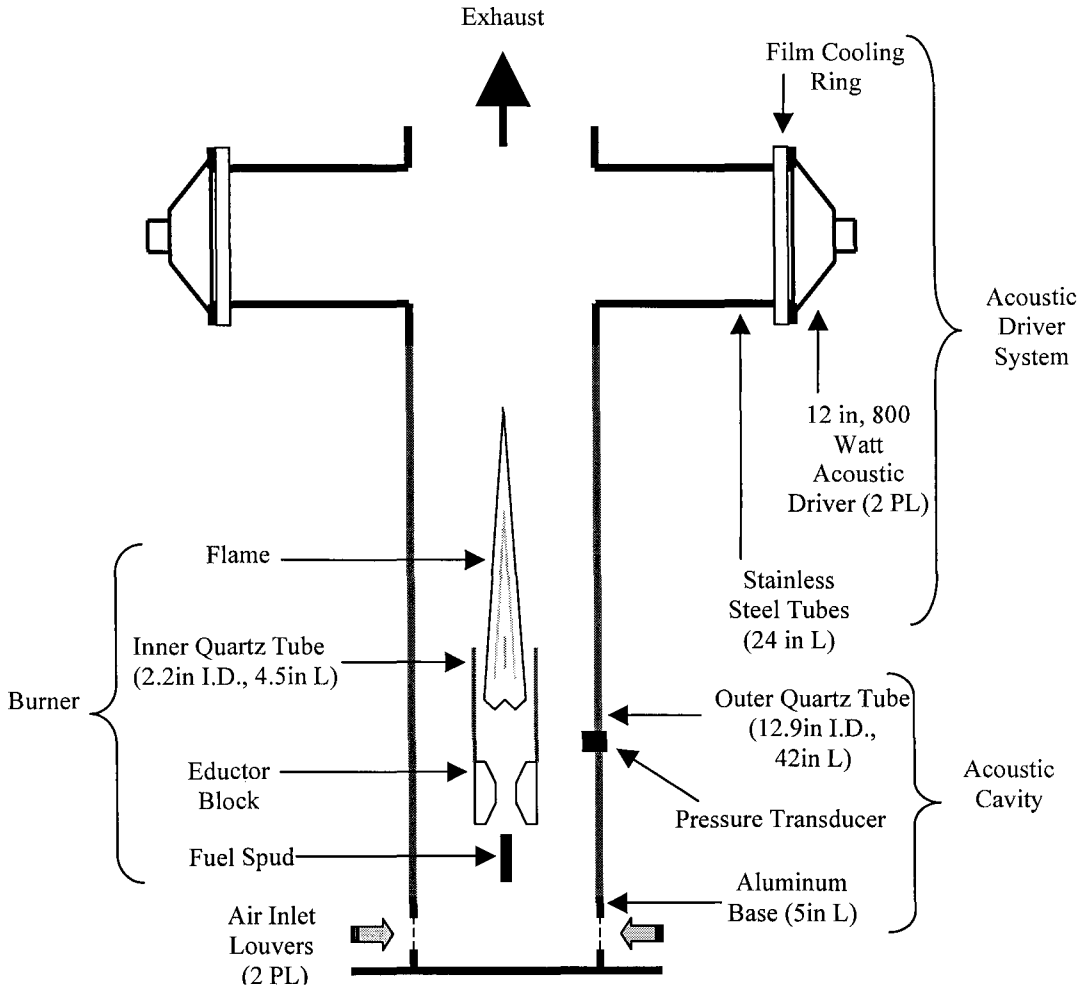

Figure 1: Schematic of Overall Test Section

Fuel for the burner is 50% methane premixed with 50% CO_2 gas to increase the mass flow. The premixer inlets for each gas are choked, in order to prevent disturbances from propagating upstream and affecting flow rates. The volumetric flow rate through the spud is 2.14 SCFM, yielding a jet velocity of 30 m/s (Re = 20,000).

A piezoelectric pressure transducer (PCB Piezotronics, model 106B50) is located at a height of 3 inches above the fuel spud, where the flame is stabilized in the burner. This transducer was selected for it's high sensitivity (493.3 mV/psi) and thermal characteristics.

A Vision Research Phantom V4.0 high-speed video camera is used to capture images during the chemiluminescence experiments. It is based on a proprietary 512 x 512 pixel monochrome SR-CMOS sensor, capable of exposure times as low as 10 μs. The camera contains 256 MB of memory on board, which allow it to acquire data at 1000 frames per second, for just over 1 second. Higher frame rates are possible by lowering the pixel resolution. The camera is equipped with a C-mount, and a Nikon 50 mm F/1.4 lens is used with a C-mount-to-F-mount adapter.

CHEMILUMINESCENCE RESULTS

Two-Dimensional Flame Structure

Single shot chemiluminescence images from the Phantom V4.0 camera were smoothed using a 3x3 median filter in Matlab. Images were then averaged by phase-locking to the pressure signal. Images were selected by locating their temporal locations, and selecting the images to be averaged based on their proximity to the sixteen phase divisions used. Approximately 15 images were used on average at each phase position. The maximum phase resolution jitter was found to be less than 2 degrees in all cases. Contours were computed and plotted for each case (five forcing frequencies x two burners) showing eight phases in a cycle. Only conditions at forcing frequencies of 22 Hz and 37 Hz are displayed in Figure 2 and Figure 3. Contour levels are plotted at 5, 20, 40, 60, 80, and 95 percent levels of the maximum intensity of the 0 degree phase contour plot for each case. In all cases, the phases are taken as a sine wave, with 0 degrees corresponding to a zero crossing with a rising edge.

For forcing at 22 Hz (Figure 2), the bluff-body burner shows a larger stabilization zone than the aerodynamic burner (40% contour), centered at approximately a height of 5 cm. Note that the center "hole" at 8 cm at a phase of 0 degrees is actually at a contour of 5%, and not 40%. Characteristics to note in both cases are the traveling of a wave in the upstream direction on the outer edge of the flame, from 0 to 180 degrees. At 180 degrees, the wave reverses itself, and travels back downstream. There is also a distinct change in intensity, as the flame oscillates. The intensity contour at 40% can be seen to grow into the burner tube as the flame evolves from 0 to 180 degrees, and in the bluff-body case even connects with the 40% contour levels in the stabilization zone. As the pressure changes from 180 to 360 degrees, these intensity zones separate from each other, and travel back downstream. These two oscillating characteristics are generally observed for each forcing frequency, except for the 55 Hz case.

At a frequency of 27 Hz, much the same phenomenon is observed, with a decrease in the amplitude of the outer propagating wave. In addition, there appears to be a superimposed higher frequency, lower amplitude outer wave, continuously traveling downstream. As the forcing frequency is increased to 32 Hz the intensity of the flame in the burner tube has diminished. Once the acoustic oscillations reach 37 Hz (Figure 3), an interesting reversal occurs. The contours in the stabilization zone show a significantly larger 40% contour for the aerodynamically stabilized burner, than the bluff-body stabilized case. Recall in all previous cases, the bluff-body stabilized burner yielded stronger stabilization zones, or at least zones comparable to that of the aerodynamically stabilized burner. Finally for the 55 Hz case there is essentially no change between contours at different phases. The low amplitude traveling waves on the outer rim of the flame are present, but none of the bulk oscillations of intensity, or flame shape that occurred in previous situations.

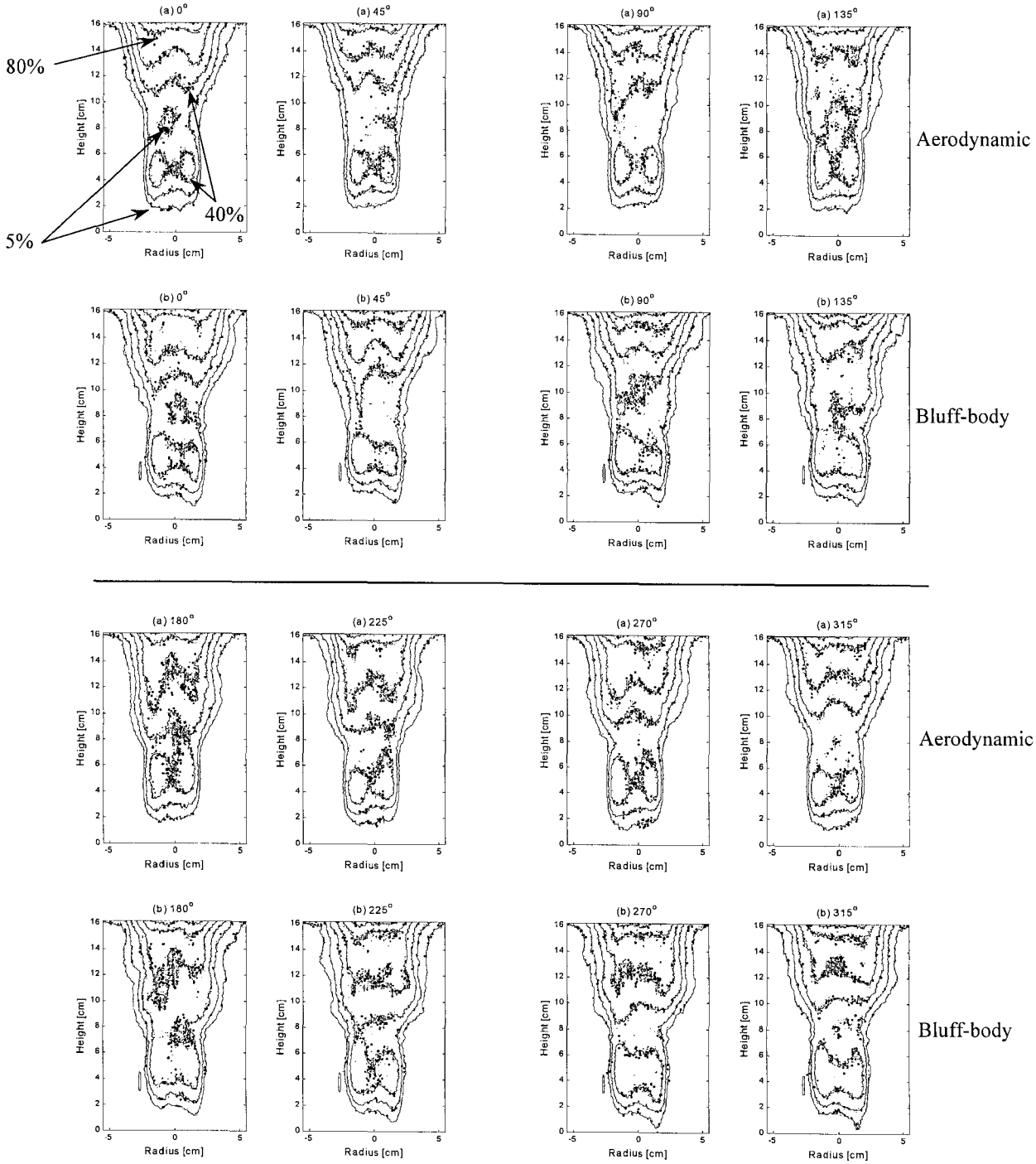

Figure 2: Chemiluminescence contour plots at 22 Hz for (a) aerodynamically stabilized and (b) bluff-body stabilized cases. Contours are at 5, 20, 40, 60, 80, and 95% of maximum intensity.

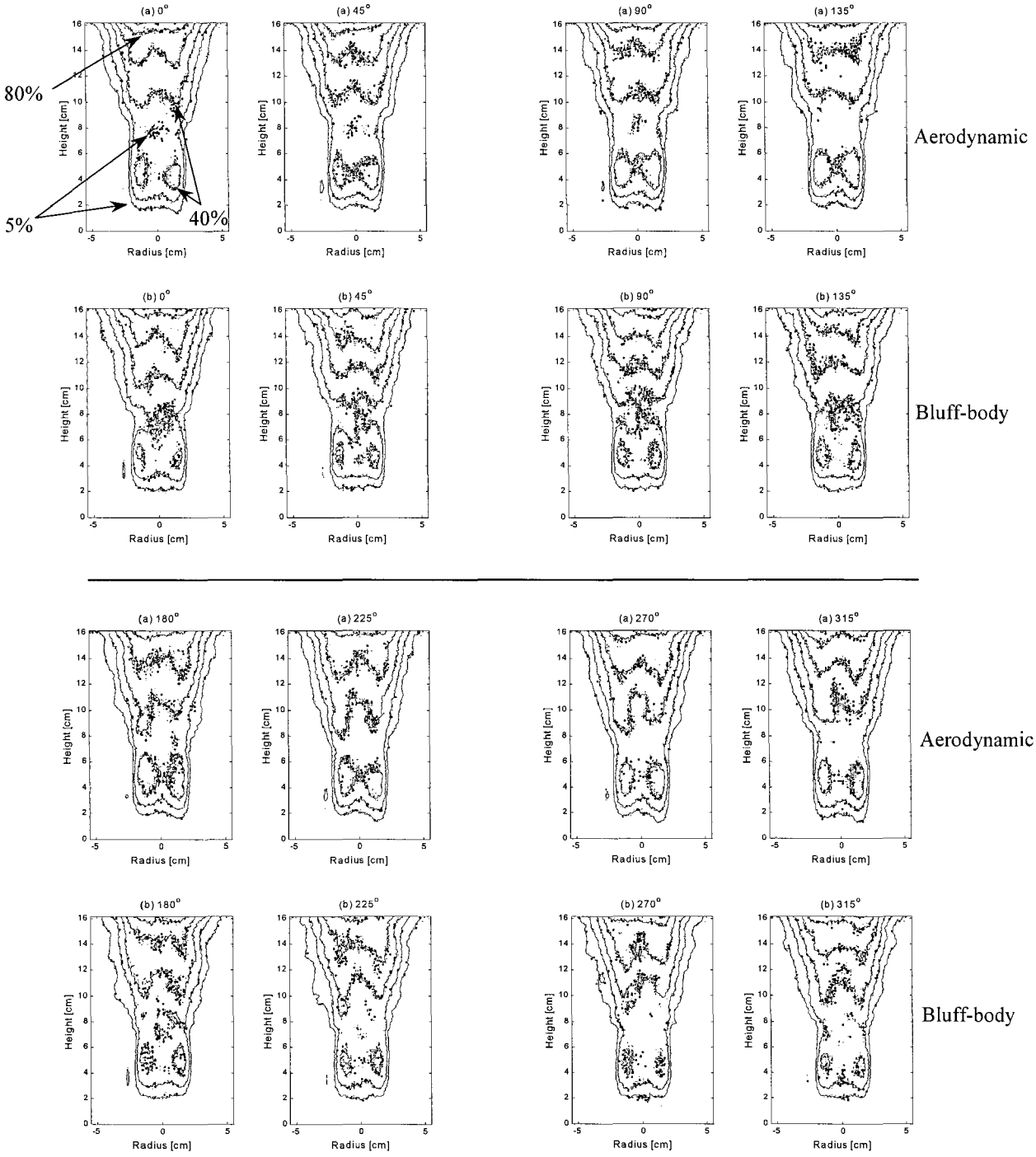

Figure 3: Chemiluminescence contour plots at 37 Hz for (a) aerodynamically stabilized and (b) bluff-body stabilized cases. Contours are at 5, 20, 40, 60, 80, and 95% of maximum intensity.

Axial Flame Structure

In order to emphasize the periodic motion contained in the flames, axial plots showing the mean intensity as a function of height and phase were constructed and plotted on a 2D contour plot (Figure 4 and Figure 5). Mean intensities were calculated using a threshold intensity of 15, corresponding to approximately 5% of the maximum intensity level in the flame. Values below the threshold were considered to be outside the flame zone, and not incorporated into the mean. In addition, the axial contours were averaged over a period, and the averages used to normalize the plots, which further enhances the periodic motion of the flame (Figure 6 and Figure 7). The mean plots of flame intensity are absolute -- they are not normalized in any way to enable comparison between different forcing conditions. The flame base is defined at an intensity level of 15, and can be easily seen on the mean axial intensity plots. Data at conditions below approximately 2 cm (below the flame base) on the normalized intensity plots should be disregarded, since they are outside the flame zone (denoted by dark blue structures). Both sets of plots cover two periods of oscillation, to emphasize the behavior.

Immediately apparent is the fluctuation of the flame base (note: the lowest intensity plotted is at 15, i.e. the flame base). In each case, the flame base oscillates in a sinusoidal manner, corresponding to the driving frequency imposed by the acoustic drivers. Table 1 compiles the mean flame height, the amplitude of the oscillation, and the percent changes of these parameters when transitioning from the aerodynamically stabilized burner to the bluff-body burner.

At low frequencies, the bluff-body stabilizer has the effect of lowering the mean flame base position. At approximately 32 Hz, a change in the characteristics of the bluff-body flame seems to occur. At frequencies greater than 32 Hz, the bluff-body case shows increased flame base positions relative to the aerodynamic case. For frequencies between 22 and 37 Hz, the flame base increases continuously, except for the aerodynamically stabilized burner, which shows a sharp lowering of the mean flame base at 37 Hz. At 55 Hz, both burners appear to enter into a regime different than the lower frequencies. In addition, the bluff-body burner generally has a lower amplitude of oscillation than the aerodynamically stabilized burner.

	Mean Height (cm)			Amplitude of Oscillation (peak-to-peak) (cm)		
Frequency (Hz)	Aero	BB	Relative Change	Aero	BB	Relative Change
22	1.65	1.17	-29%	0.89	1.02	+15%
27	1.88	1.25	-33%	0.56	0.40	-28%
32	2.07	1.90	-8%	0.55	0.24	-56%
37	1.53	2.14	+40%	0.50	0.28	-44%
55	0.37	1.06	+186%	0.14	0.16	+14%

Table 1: Flame base position and oscillation.

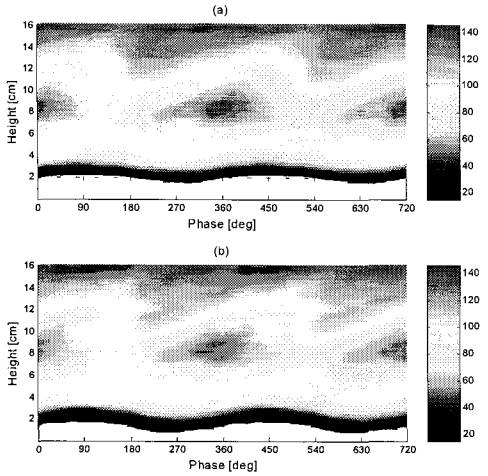

Figure 4: Mean axial intensities at 22 Hz (a) aerodynamic (b) bluff-body.

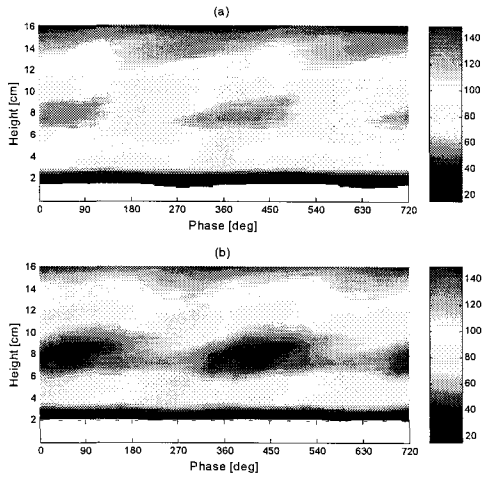

Figure 5: Mean axial intensities at 37 Hz (a) aerodynamic (b) bluff-body.

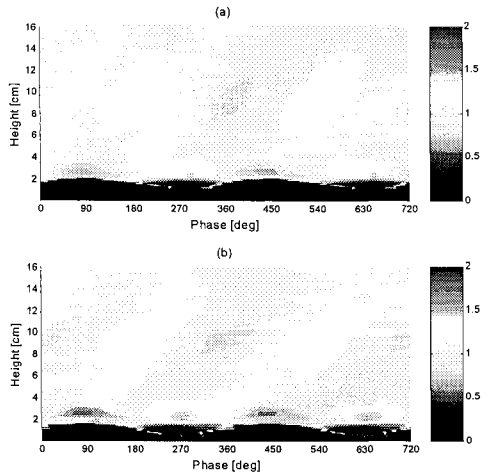

Figure 6: Normalized axial intensities at 22 Hz (a) aerodynamic (b) bluff-body.

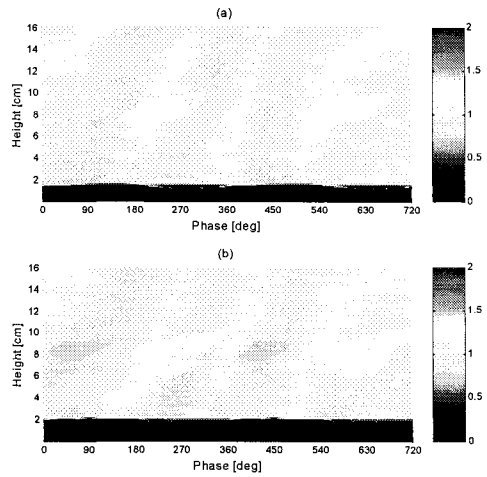

Figure 7: Normalized axial intensities at 37 Hz (a) aerodynamic (b) bluff-body.

Figure 4 and Figure 6 show the mean and normalized axial intensities at 22 Hz. It is evident from the flame structure that both burners are responding strongly to the acoustic forcing. The ranges of motion taken from the normalized axial intensity are comparable in size, with the aerodynamic burner tending to oscillate at a higher overall position. Note the higher angle of oscillation for the aerodynamic case in Figure 6. This implies a larger velocity of the flame, possibly due to flow retardation caused by the enhanced recirculation off the bluff-body burner. The 22 Hz case is typical for frequencies ranging up to 32 Hz.

At 37 Hz, again the system is observed to contain a different dynamical response compared to the lower frequencies. There is much stronger anchoring of the flame in the aerodynamic case at the flame base, as shown in Figure 5 when compared against the bluff-body case. This is the opposite of observations at lower frequencies. Figure 7 shows significantly more motion

in the bluff-body case, which is again observed for the first time. At a frequency of 55 Hz, there is essentially no response by the flame to the acoustic forcing.

SUMMARY

Chemiluminescence provided measures of the flame base location at different forcing frequencies, and gave a measure of the difference in response between the aerodynamically stabilized and bluff-body stabilized burners. In general, the bluff-body burner lowered the position of the flame base, except at 37 Hz, where the opposite effect was observed. Lowering of the flame base appears to correlate well with increased flame stiffness and stability of the system viewed under Rayleigh's criteria. These results agree with tests on the same configuration using OH PLIF to determine Rayleigh Indices (Pun, et al., 2000), and may be a possible indicator for improved stability characteristics without the need to turn to more complicated laser diagnostics. Results at 55 Hz showed very little response in the flame due to the acoustic excitation. It appears that the burners enter a different regime when they are excited at 55 Hz, though this result could be misleading and will be verified by tests at higher frequencies.

REFERENCES

Broda, J.C., Seo, S., Santoro, R.J., Shirhattikar, and Yang, V. (1998) "An Experimental Study of Combustion Dynamics of a Premixed Swirl Injector", Twenty-Seventh Symposium (International) on Combustion, The Combustion Institute.

Chen, T.Y., Hegde, U.G., Daniel, B.R., and Zinn, B.T. (1993) "Flame Radiation and Acoustic Intensity Measurements in Acoustically Excited Diffusion Flames", J. Propul. Power, Vol. 9, No. 2.

Hurle, I.R., Price, R.B., Sugden, T.M., and Thomas, A., (1968) "Sound Emission from Open Turbulent Premixed Flames", Proc. Roy. Soc., Vol. 303, pp. 409-427.

Kendrick, D.W., (1995) "An Experimental And Numerical Investigation Into Reacting Vortex Structures Associated With Unstable Combustion", Ph.D. Thesis, California Institute of Technology, Pasadena, CA.

McManus, K., Yip, B., and Candel, S., (1995) "Emission and Laser-Induced Fluorescence Imaging Methods in Experimental Combustion", Experimental Thermal and Fluid Science, Vol. 10, pp. 486-502.

Pun, W., Palm, S.L., and Culick, F.E.C. (2000) "PLIF Measurements of Combustion Dynamics in a Burner under Forced Oscillatory Conditions" AIAA-2000-3123, *presented at the 36th Joint Propulsion Conference*, Huntsville, AL.

Samiengo, J.M., Yip, B., Poinsot, T., and Candel, S., (1993) "Low-Frequency Combustion instability Mechanisms in a Side-Dump Combustor", Combustion and Flame, Vol. 94, Iss. 4, pp. 363-380.

Shih, W.P, Lee, J.G., and Santavicca, D.A., (1996) "Stability and Emissions Characteristics of a Lean Premixed Gas Turbine Combustor", Twenty-Sixth Symposium (International) on Combustion, The Combustion Institute.

Sterling, J.D., (1987) "Longitudinal Mode Combustion Instabilities in Air Breathing Engines", Ph.D. Thesis, California Institute of Technology, Pasadena, CA.

Zsak, T.W. (1993) "An Investigation of the Reacting Vortex Structures Associated with Combustion", Ph.D. Thesis, California Institute of Technology, Pasadena, CA.